

Marquette University

**e-Publications@Marquette**

---

Computer Science Faculty Research and  
Publications

Computer Science, Department of

---

7-2020

## **Chance-Constrained Optimization of Energy Storage Capacity for Microgrids**

Nasim Yahyasoltani

Adel Nasiri

Follow this and additional works at: [https://epublications.marquette.edu/comp\\_fac](https://epublications.marquette.edu/comp_fac)

---

Marquette University

**e-Publications@Marquette**

***Computer Science Faculty Research and Publications/College of Arts and Sciences***

***This paper is NOT THE PUBLISHED VERSION.***

Access the published version via the link in the citation below.

*IEEE Transactions on Smart Grid*, Vol. 11, No. 4 (2020): 2760-2770. [DOI](#). This article is © Institute of Electrical and Electronics Engineers (IEEE) and permission has been granted for this version to appear in [e-Publications@Marquette](#). Institute of Electrical and Electronics Engineers (IEEE) does not grant permission for this article to be further copied/distributed or hosted elsewhere without the express permission from Institute of Electrical and Electronics Engineers (IEEE).

# Chance-Constrained Optimization of Energy Storage Capacity for Microgrids

Nasim Yahya Soltani

Department of Computer Science, Marquette University, Milwaukee, WI

Adel Nasiri

Center for Sustainable Electrical Energy Systems, University of Wisconsin-Milwaukee, WI

## Abstract

The optimal storage capacity is a crucial parameter for stable and reliable operation of microgrids in an islanded mode. In this context, an analytical method is developed to robustly formulate and analyze energy storage capacity deploying chance constrained stochastic optimization. More specifically, the goal is to determine an appropriate size for an energy storage to reach a specific loss of load probability (LOLP) in a microgrid with large penetration of renewables considering generation and load forecast error. The total cost is minimized over optimal storage capacity as well as over generators power, while accounting for generation and storage power and energy constraints. It is postulated that the shortage/surplus power will be derived from/injected to the

storage system. However, due to stochastic nature of load and renewables and an inevitable forecast error, the renewable generation output or the load power may not be accurately acquired. Thus, the total storage power and energy constraints are posed as chance constraints, for which conservative convex approximations are employed for tractability. In particular, to overcome the difficulty brought about by the large size of the optimization problem, a separable (distributed) structure is pursued, and the dual decomposition method is adopted to obtain optimal solutions. Numerical tests verify the effect of prior knowledge in modeling the uncertainty in optimal choice of storage capacity.

## Nomenclature

### Abbreviation Expansion

$S_k^t$	The stored energy at time $t$ in the battery $k$
$P_k^{min}, P_k^{max}$	Minimum and maximum charge/discharge power for $k$ th battery
$P_k^t$	The amount of charge/discharge power for each battery $k$ at time $t$
$P_{G_d}^t$	The instantaneous power output of the generator $d$ at time $t$
$P_{excess}$	The amount of power curtailment for renewable sources in order to limit the charging power of the battery
$\alpha_k, \beta_k$	Coefficients for battery $k$ cost function
$C_E^t$	Total operational cost of energy storage system at time $t$
$L_1^t, L_2^t, L_3^t, L_4^t$	Lagrangian functions
$\mu_t^-, \mu_t^+, \sigma_t$	Constants
$\sigma_Z^t$	Variance of $Z^t$
$\epsilon$	Probability violation threshold
$\zeta_Z^t$	Auxiliary variable at time $t$
$a_Z^t, b_Z^t$	Auxiliary variables at time $t$
$A^t, B^t, V^t, H^t$	Auxiliary variables at time $t$
$C_k^t$	Cost of energy storage $k$ at time $t$
$C_R^t$	Covariance matrix of the renewables forecast error at time $t$
$D$	Number of synchronous generators
$DoD_k^{th}$	Maximum allowable depth of discharge for battery $k$
$\nu, \omega, \gamma$	Vectors of dual variables
$K$	Number of storage devices
$M$	Number of renewable generators
$N$	Number of consumers with different types of loads
$P_{cap}$	Power threshold to adjust variations of battery charging power
$P_E^t, S_E^t, C_E^t$	Total storage, charging/discharging power and cost of storage system at time $t$
$P_G^{min}, P_G^{max}$	Minimum and maximum allowable generation power
$\hat{P}_{L_{net}}^t$	The load forecast of $N$ consumers at time $t$
$\tilde{P}_{R_m}^t$	The renewable generation $m$ output power forecast at time $t$
$\bar{P}_{L_{net}}^t$	The load forecast error of $N$ consumers at time $t$
$P_{L_{net}}^t$	Aggregate power consumption of $N$ consumers at time $t$
$P_{R_m}^t$	The renewable generation $m$ output power at time $t$
$\hat{P}_{R_m}^t$	The renewable generation $m$ output power forecast at time $t$
$(\sigma_{L_{net}}^t)^2$	Variance of the load forecast error at time $t$
$(\sigma_{R_{net}}^t)^2$	Variance of the renewables forecast error at time $t$
$(\sigma_Z^t)^2$	Variance of shortage output at time $t$

$S_k^{min}, S_k^{max}$	Minimum and maximum storage capacity for battery $k$
$S_k^{th}$	Stored energy allowable threshold for battery $k$
$g_v^t, g_\omega^t, g_\gamma^t$	Subgradients <i>w. r. t.</i> $v, \omega, \gamma$
$U^t$	The instantaneous shortage or surplus power to meet the microgrid demand balance at time slot $t$
$Z^t$	Auxiliary variable as shortage output
$\zeta_k \in (0, 1]$	The charging/discharging efficiency of the $k$ th battery.

## SECTION I. Introduction

The Microgrid vision is on extending distributed energy resources (DER) and reducing the losses from long-distance transmission for a more reliable and efficient power network and greener environment. The term DER entails distributed storage system (DSS), renewable generation and fuel-based generators. Through DER a microgrid can enhance the reliability as well as other environmental and economical benefits.

There are two modes of operation for microgrids. Microgrids can operate stand alone in islanded mode or be connected to the main grid in a grid-connected mode. Specially in islanded mode and with pertinent goal of minimal fuel-based generation, an uninterrupted and stable microgrid operation is ensured through an energy storage system (ESS). Specifically, with a high penetration of renewables, the availability of such energy resources involve uncertainty and calls for advanced planning and scheduling [1], [2], [3], [4], and [5].

One of the applications of ESS is to accommodate for the variabilities of intermittent energy sources such as wind and solar generation. Therefore, to meet the total demand at each time instant, one needs to plan to save some of the excess generated energy for later use through an ESS [6].

Pre-requisite to optimal generation and ESS sizing tasks is a reliable load and renewable generation forecast. Due to stochastic nature of the renewable power generation and sudden variation of the load, the task of forecast is challenging. Obviously, a long-term (month-ahead) forecast data entail more error than the short-term (hours-ahead or day-ahead) prediction. Specifically, a couple of approaches are often employed to capture uncertainty [7]. Statistical knowledge of the uncertain parameters such as the mean and covariance, or the distribution may be assumed, which leads to chance-constrained formulations. An alternative is to adopt a robust optimization framework, where a bounded uncertainty region is postulated.

Power and energy constraints under generation/load uncertainty can be cast as chance constraints [8], [9], [10], [11]. However, chance constraints are typically more difficult to handle than their deterministic counterparts, as they may be either non-convex, or tough to verify as being convex. Moreover, it is sometimes difficult to express these constraints in closed form. In such cases, convex approximation of the chance constraints is of practical merit [12], [13].

The problem of ESS sizing with different potential purposes including balancing the variations of the intermittent resources have been extensively addressed in the literature [4], [5], [14], [15]. However, only a limited number of papers have considered the forecast error and uncertainty in the problem formulation [8], [16], [17], [18], [19]. The wind power forecast errors obtained from persistence scenarios were used in [16] for ESS sizing. In [17], incorporating spatiotemporal interdependencies, a stochastic model of the wind is proposed to obtain the size of ESS. While, taking into account the uncertainty from renewable resources and dynamic pricing of the electricity, optimal sizing and management of ESS is addressed using dynamic programming in [18]. In [19] a sharing-based energy storage system to manage the peak hour energy for residential customers is proposed where the demand of each customer is modeled stochastically. The power shortage has been modeled through a probabilistic constraint in [8], and the optimal size of the ESS, the

renewables and synchronous generators were obtained, where the probabilist shortage constraint was handled using scenario approximation.

Electrical microgrids are experiencing a large growth due to three reasons: 1) reduction in cost of solar PV; 2) decreasing cost of electrical storage; and 3) lower cost for smaller natural gas generators. Microgrids provide higher energy efficiency, higher reliability and lower cost to customers. Microgrids generally include a large share of renewable energy systems which are naturally intermittent. Energy storage systems are generally required for management of energy, voltage, and frequency in order to not significantly oversize non-renewable generations. All microgrids use energy storage systems in one form or another. This work enables optimization of energy storage system size in order to reduce the overall cost of microgrids. The impact of the proposed work is significant as microgrid systems are very cost-sensitive due to novelty of the technology. Major developments of microgrids have been for campuses (universities, hospitals, military installations), where there is demand for lower energy cost and higher reliabilities. Microgrids have also found very niche applications, for instance to power residential areas (especially in California) when grid power is frequently out due to wild fire hazards. For all these applications, there is a need for advanced optimization of energy storage size and capacity to meet the requirements.

The present paper addresses the joint storage capacity and generation optimization task in islanded microgrid with uncertain renewable generation and load power. An expected cost minimization problem is formulated under the maximum and minimum allowable generation power and storage capacity constraints as well as the probabilistic power and energy constraints to guarantee a stable operation of the microgrid. The Bernstein method with minimal prior knowledge of the uncertain parameter is adopted to approximate the probabilistic constraints by convex and conservative surrogates. The resultant algorithm is then compared with Gaussian approximation as well as the case where load and renewables forecast errors are fully ignored. It will be shown that using those approximations the resultant problem is convex and separable per time slot, which opens the door to the dual decomposition approach, which leads to an optimal, distributed and computationally efficient solution with performance guarantee

Compared to the existing literature, the contribution of this paper is fourfold, and of critical importance for microgrids with high-penetration of renewables. First, a detailed model for storage cost functions including battery lifetime is incorporated in the optimization problem. Second, both load and wind power uncertainty is modeled and captured not only in the constraints but also in the objective function. Third, in addition to analytical modeling of the uncertainty in the forecast error through Gaussian approximation, the current work will also explore the case where there is no prior knowledge on the probability distribution function of the forecast error and proposes a novel approach with an analytical and closed-form expression to handle such cases. Finally, since looking at a large historical data for storage sizing is computationally expensive, a solid, distributed, and efficient algorithm with performance guarantee is proposed to effectively solve the robust sizing problem. Detailed numerical tests are presented to illustrate the effects of different approaches in capturing uncertainty in ESS sizing problem.

The rest of the paper is organized as follows. The problem is introduced and formulated in Section II and Section III. Bernstein's approximation and Gaussian approximation techniques tailored for chance constraints are outlined in Section IV. The robust and deterministic algorithms are developed in Section V. Numerical tests are presented in Section VI, followed by conclusions in Section VII.

*A Note on Notations:* In this paper, vector quantities are denoted as bold letters, and the sets as calligraphic upper-case letters. Superscript<sup>t</sup> as in  $P_G^{(t)}$  denotes the quantities related to the  $t$ -th time slot and  $Pr\{\cdot\}$  represents the probability.

## SECTION II. System Components

Consider a microgrid comprising of N consumers with different types of loads, M renewable generators, and K storage devices.

### A. Demand Profile

Let  $P_{L_{net}}^t$  indicate the aggregate power consumption of N consumers at time  $t$ ; i.e.,  $P_{L_{net}}^t$  is a continuous random variable.

Let  $\hat{P}_{L_{net}}^t$  denote the load forecast of the consumers at time  $t$ . Then, the aggregate power consumption can be written as

$$P_{L_{net}}^t = \hat{P}_{L_{net}}^t + \tilde{P}_{L_{net}}^t \quad (1)$$

where  $\tilde{P}_{L_{net}}^t$  is a zero-mean random variable with variance  $(\sigma_{L_{net}}^t)^2$  capturing the forecast error and consumption dependencies of consumers. A typical choice of  $\tilde{P}_{L_{net}}^t$  is Gaussian.<sup>1</sup> However, in general the probability distribution of  $\tilde{P}_{L_{net}}^t$  depends on the forecast method.

### B. Energy Storage Model

It is assumed that the microgrid is using an energy storage system including a set of electrochemical batteries represented by  $\mathcal{K}$ , where  $|\mathcal{K}| = K$ . Let  $S_k^t$  and  $P_k^t$  denote the stored energy and charging/discharging power at time  $t \in \tau \triangleq \{1, 2, \dots, T\}$  in the battery  $k \in \mathcal{K}$ , respectively. With  $\zeta_k \in (0, 1]$  as the average round trip efficiency of the battery  $k$ , the stored energy of battery  $k$  at time slot  $t$  can be written as

$$S_k^t = S_k^{t-1} + \zeta_k P_k^t, \quad k \in K \quad (2)$$

Where  $P_k^t > 0$  when charging and  $P_k^t < 0$  during discharge period. In general, to protect battery life a minimum allowable energy,  $S_k^{min}$  is set. With  $S_k^{max}$  as the maximum storage capacity, the storage capacity of battery  $k$  is bounded as

$$S_k^{min} < S_k^t < S_k^{max}, \quad k \in K \quad (3)$$

Similarly, the amount of charge/discharge power for each battery is constrained by

$$P_k^{min} < P_k^t < P_k^{max}, \quad k \in K \quad (4)$$

To increase lifetime of the battery, it is recommended that the stored energy does not get below a specified threshold,  $S_k^{th} := (1 - DOD_k^{th})S_k^{max}$ , where superscript th refers to 'threshold' and  $DOD_k^{th}$  represents the maximum allowable depth of discharge for battery  $k$ . Then, the cost of energy storage at time slot  $t$  can be formulated as

$$C_k^t = \alpha_k S_k^{max} + \beta_k^t (S_k^{th} - S_k^t), \quad k \in K \quad (5)$$

where the first term refers to investment cost and the second term captures the operational cost which is proportional to the variation in battery energy (rate of charge and discharge) [20].

One can then easily obtain the total storage capacity,  $S_E^t$ , charge/discharge power,  $P_E^t$ , and the total cost of the storage system,  $C_E^t$  as follows

$$S_E^t = \sum_{k=1}^K S_k^t, \quad P_E^t = \sum_{k=1}^K P_k^t \quad (6)$$

$$C_E^t = \sum_{k=1}^K \alpha_k S_k^{max} + \sum_{k=1}^K \beta_k^t (S_k^{th} - S_k^t) \quad (7)$$

The constrains (3), (4), and (5) for the total storage system are then given by

$$S^{min} < S_E^t < S^{max} \quad (8)$$

$$P_E^{min} < P_E^t < P_E^{max} \quad (9)$$

where

$S^{min} := \sum_{k=1}^K S_k^{min}$ ,  $P_E^{max} := \sum_{k=1}^K P_k^{max}$ , and  $P_E^{min} := \sum_{k=1}^K P_k^{min}$ . With  $S^{max} := \sum_{k=1}^K S_k^{max}$  and the choices of  $\alpha_{max} = \max\{\alpha_k\}_{k=1}^K$ , and  $\beta_{max}^t = \max\{\beta_k^t\}_{k=1}^K$ , the total operational cost of energy storage system at time t is upper-bounded by

$$C_E^t \leq \alpha_{max} S^{max} + \beta_{max}^t [(1 - DoD^{th}) S^{max} - S_E^t] \quad (10)$$

Usually, smaller variation of energy promotes longer battery lifetime and efficiency. Clearly, higher values of  $\beta_{max}^t$  allow for smaller variations of the stored energy. If  $K=1$  and one large storage is considered, then  $\beta_{max}^t$  is replaced by  $\beta_1^t$ .

### C. Renewable Generation Model

The set of renewable power generators consisting of wind turbines and photovoltaics (PV) is represented by  $\mathcal{R}$  where  $|\mathcal{R}| = M$ . Let  $P_{R_m}^t$  denote the instantaneous power output of Wind turbine or PV generation  $m \in \mathcal{R}$  at time  $t$ . For instance, the amount of power generated by a wind turbine varies with wind speed. Using the historical data, the wind turbine output power versus wind speed curve (power-speed curve) can be predicted, i.e., for wind turbine  $m$  at time  $t$  given the wind speed,  $v^t$ , the output power,  $\hat{P}_{R_m}^t$  is obtained. Similarly, PV output power forecast can be obtained. The power output of the renewable generation source  $m$ ,  $P_{R_m}^t$ , can then be defined as a deterministic mean (or “nominal” value) plus a perturbation (error) term as follows

$$P_{R_m}^t = \hat{P}_{R_m}^t + \tilde{P}_{R_m}^t \quad m = 1, \dots, M \quad (11)$$

where  $\hat{P}_{R_m}^t$  denotes a typical power output, obtained from forecast and  $\tilde{P}_{R_m}^t$  accounts for forecast error at time  $t$ . Let  $\hat{\mathbf{P}}_R^t$  and  $\tilde{\mathbf{P}}_R^t$  collect all  $\hat{P}_{R_m}^t$  and  $\tilde{P}_{R_m}^t$ , respectively, i.e.,  $\hat{\mathbf{P}}_R^t := [\hat{P}_{R_1}^t, \dots, \hat{P}_{R_M}^t]$  and  $\tilde{\mathbf{P}}_R^t := [\tilde{P}_{R_1}^t, \dots, \tilde{P}_{R_M}^t]$ . It is also postulated that the forecast error is zero mean with a known covariance matrix  $C_R^t$ . Then, the probability distribution function (*p.d.f*) of  $P_R^t$  can be represented by  $P_R^t \sim f(\hat{\mathbf{P}}_R^t, C_R^t)$ , where  $f(\cdot)$  may in general be unknown. For notational simplicity, and without loss of generality (w.l.o.g), one can define the net renewable generation

as  $P_{R_{net}}^t := \sum_{m=1}^M P_{R_m}^t$ . The first and second order statistics of  $P_{R_{net}}^t$  can then be written as

$$\mathbb{E}\{P_{R_{net}}^t\} = \sum_{m=1}^M \hat{P}_{R_m}^t \quad (12)$$

$$(\sigma_{R_{net}}^t)^2 = \sum_{m=1}^M \sum_{n=1}^{m-1} \{[C_R^t]_{mm} + 2[C_R^t]_{mn}\} \quad (13)$$

With  $(\sigma_{R_{net}}^t)^2$  as the variance of  $P_{R_{net}}^t$ , it holds that  $P_{R_{net}}^t \sim h(\hat{P}_{R_{net}}^t (\sigma_{R_{net}}^t)^2)$ , where the function  $h(\cdot)$  can in general be assumed an unknown p.d.f.

#### D. Synchronous Generator

The set of synchronous generators is represented by  $\mathcal{D}$  where  $|\mathcal{D}| = D$ . Let  $P_{G_d}^t$  denote the instantaneous power output of the generator  $d \in \mathcal{D}$  at time  $t \in \{1, \dots, T\}$  and  $\mathbf{P}_G^t := [P_{G_1}^t, \dots, P_{G_D}^t]$ , then  $P_{G_d}^t$  follows a box constraint as

$$P_G^{min} \leq P_{G_d}^t \leq P_G^{max} \quad d \in D, t \in \tau \quad (14)$$

where  $P_G^{min}$  and  $P_G^{max}$  represent the minimum and maximum allowable generation power. The generation cost is typically modeled as a convex and quadratic function in total power  $P_{G_d}^t$  as  $a_d P_{G_d}^t{}^2 + b_d P_{G_d}^t + c_d$ , where  $a_d, b_d, c_d$  are constants.

#### E. Demand Balance Constraint

Suppose microgrid is operating in islanded-mode. Then, the total generation must meet the total demand and the energy shortage is supplied by the battery. Similarly, the excess generation can be stored in the battery for later use. It is desirable to have the renewable generation at the maximum foretasted capacity. However, in a condition with very light load and high renewable generation, parameter  $P_{excess}^t$  is defined as the amount of power curtailment for renewable sources in order to limit the charging power of the battery under its nominal rating and avoid an storage system with an unreasonably large capacity. Also,  $\mathbf{P}_{excess}$  collects  $P_{excess}^1, \dots, P_{excess}^T$ . The instantaneous shortage or surplus power to meet the microgrid demand balance at time slot  $t$  can then be defined as

$$U^t := P_{R_{net}}^t + \sum_{d=1}^D P_{G_d}^t - P_{L_{net}}^t - P_{excess}^t \quad (15)$$

Clearly,  $U^t < 0$  denotes the shortage in the microgrid which needs to be supplied by the storage system and  $U^t > 0$  represents the surplus power stored in the storage system.

### SECTION III. Energy Storage Capacity Optimization

The cost efficient operation of a microgrid in islanded-mode calls for maximum generation of renewables and minimum supply from the synchronous generators. In addition, the demand balance constraint in (15) ensures that the total demand is satisfied, thus guaranteeing an stable operation of the microgrid. Furthermore, the energy and power requirements of the storage system must be met. Let define  $Z^t := P_{R_{net}}^t - P_{L_{net}}^t$  for notational and computational simplicity. Then, the storage capacity optimization problem amounts to

$$\begin{aligned}
\text{(P1)} \quad & \min_{S^{max}, P_{excess}, P_G^t} \sum_{t=1}^T \sum_{d=1}^D (a_d P_{G_d}^t + b_d P_{G_d}^t + c) \\
& + \mathbb{E} \left\{ \sum_{t=1}^T \beta_{max}^t \left[ (1 - DoD^{th}) S^{max} - \sum_{t'=1}^t U^{t'} \right] \right\} \\
& + \eta^t \mathbb{E} \left\{ \sum_{t=1}^T (Z^t - P_{excess}^t - P_{cap})^2 + \alpha S^{max} \right\} \\
\text{subject to:} \quad & \Pr \left( S^{min} \leq S_E^0 + \sum_{t'=1}^t U^{t'} \leq (1 - DoD^{th}) S^{max} \right) \\
& \geq 1 - \epsilon, t \in \tau \\
& \Pr(P_E^{min} \leq U^t \leq P_E^{max}) \geq 1 - \epsilon, t \in \tau \\
& P_G^{min} \leq P_{G_d}^t \leq P_G^{max}, d \in D, t \in \tau \\
& \mathbf{0} \leq P_{excess}^t \\
& 0 \leq S^{max} \leq S^{cap}
\end{aligned}$$

where the objective function is the expected cost incurred by the stochastic charge/discharge power over the varying renewable output power and load power, i.e., the expectation is with respect to  $Z^t$  ( $P_{R_{net}}^t$  and  $P_{L_{net}}^t$ ). The third term in the cost function is to adjust variations of battery charging power and encourage the battery charging power to remain below a specified level denoted as  $P_{cap}$ . This soft constraint avoids an unreasonably large energy storage system. Clearly, higher weights,  $\eta$  lead to smaller variations. The probability that total battery energy at each time does not violate the maximum/minimum battery capacity is limited by  $1 - \epsilon$  in (17) and (18) ensures that the probability that the battery power flow goes beyond the pre-specified limits does not exceed  $1 - \epsilon$ . Constraint (19) limits the minimum/maximum synchronous generator power output. Similarly, constraints (20) and (21) are the required box constraints for  $P_{excess}$  and  $S^{max}$ , respectively. It is natural to assume that the uncertainty involved in renewable generation is independent of the load uncertainty, i.e.,  $P_{R_{net}}^t \perp\!\!\!\perp P_{L_{net}}^t$  for  $t \in \tau$ . Upon the load and renewable generation output power independence, the expectation terms in (16) can be re-written as

$$\begin{aligned}
& \sum_{t=1}^T \beta_{max}^t \left[ (1 - DoD^{th}) S^{max} - \sum_{t'=1}^t \mathbb{E}\{U^{t'}\} \right] \\
& + \mathbb{E}\{(Z^t)^2\} - 2(P_{cap} + P_{excess}^t) \mathbb{E}\{Z^t\} + (P_{excess}^t + P_{cap})^2 \quad (22)
\end{aligned}$$

where  $U^t$ ,  $\mathbb{E}\{U^t\}$  can be expressed as

$$U^t = \sum_{d=1}^D P_{G_d}^t + Z^t - P_{excess}^t \quad (23)$$

$$\mathbb{E}\{U^t\} = \sum_{d=1}^D P_{G_d}^t + \hat{P}_{R_{net}}^t - \hat{P}_{L_{net}}^t - P_{excess}^t \quad (24)$$

Also,  $\mathbb{E}\{(Z^t)^2\} = (\sigma_{R_{net}}^t)^2 + (\sigma_{L_{net}}^t)^2 + (\hat{P}_{L_{net}}^t)^2 + (\hat{P}_{R_{net}}^t)^2 - 2\hat{P}_{L_{net}}^t \hat{P}_{R_{net}}^t$

Upon substituting  $U^t$  from (23) the probabilistic constraint in (17) is represented by

$$\Pr \left( 0 \leq -S^{min} + S_E^0 + \sum_{t'=1}^t \left( Z^{t'} + \sum_{d=1}^D P_{G_d}^{t'} \right) \leq (1 - DoD^{th})S^{max} - S^{min} \right) \geq 1 - \epsilon$$

and can alternatively be substituted by the following two constraints as

$$\Pr \left( \begin{aligned} & -(1 - DoD^{th})S^{max} + S_E^0 + \sum_{t'=1}^t \left( Z^{t'} + \sum_{d=1}^D P_{G_d}^{t'} \right) \leq 0 \\ & \geq 1 - \frac{\epsilon}{2} \end{aligned} \right) \quad (25)$$

and

$$\Pr(S^{min} - S_E^0 - \sum_{t'=1}^t Z^{t'} - \sum_{t'=1}^t \sum_{d=1}^D P_{G_d}^{t'} \leq 0) \geq 1 - \frac{\epsilon}{2} \quad (26)$$

Similarly, constraint  $\Pr(P_E^{min} \leq U^t \leq P_E^{max}) \geq 1 - \epsilon$  can be splitted as

$$\begin{aligned} \Pr \left( Z^t + \sum_{d=1}^D P_{G_d}^t - P_E^{max} \leq 0 \right) &\geq 1 - \frac{\epsilon}{2} \\ \text{and } \Pr \left( P_E^{min} - Z^t - \sum_{d=1}^D P_{G_d}^t \leq 0 \right) &\geq 1 - \frac{\epsilon}{2} \end{aligned} \quad (27) \quad (28)$$

For notational simplicity, let  $\epsilon' := \frac{\epsilon}{2}$ .

Remark 1:

The new probabilist constraints in (25)–(26) and (27)–(28) can conservatively substitute their original counterparts in (17) and (18). To verify that, let for example  $\Pr\{A < x < B\} > 1 - \epsilon$  which is equivalent to  $P(x > A) + P(x < B) - 1 > 1 - \epsilon$ . Therefore, the following  $P(x > A) + P(x < B) > 2 - \epsilon$  holds. Substituting the above equation with  $P(x > A) > 1 - \epsilon/2$ , and  $P(x < B) > 1 - \epsilon/2$  follows  $P(x > A) + P(x < B) > 2 - \epsilon$ .

It is worth noting that in general, the feasible set of (17) and (18) can be either convex or non-convex, depending on the distribution of random parameters  $Z^t$ . However, even if the constraints are convex, it may not be straightforward to express them in closed form, rendering the optimization problem intractable. A useful approach to tackle the non-convexity and non-tractability of the chance constraints, is to substitute the constraint with a convex and conservative surrogate. To this end, Gaussian and Bernstein approximation are deployed and introduced in Section IV.

## SECTION IV. Convex Approximation of Chance Constraints

### A. Bernstein Approximation

With no knowledge on probability distribution of  $Z^t$ , except the mean and variance, we would like to replace chance constraints in problem (P1) with convex and tractable approximations. In addition, the surrogate constraints need to be conservative, in the sense that the feasible set of approximate constraints are a subset of

the original chance constraints. Therefore, the optimal solution of the approximate problem will be a feasible suboptimal solution of (P1). A special class of convex conservative approximation techniques for chance constraints includes Bernstein approximations which is briefly reviewed in the present context [7], [21]. Consider a chance constraint of the form

$$Pr \left\{ f^0(\mathbf{x}) + \sum_{t=1}^T \zeta^t f^t(\mathbf{x}) < 0 \right\} \geq 1 - \epsilon \quad (29)$$

where  $x$  is a deterministic parameter vector, and  $\{\zeta_n\}$  are random variables with marginal distributions denoted as  $\{\pi_n\}$ . The following assumptions are necessary to deploy the approximation.

1.  $\{f^n(x)\}$  are affine in  $\mathbf{x}$  for  $t = 0, 1, \dots, T$ ;
2.  $\{\zeta^t\}$  are independent of each other; and
3.  $\{\pi^t\}$  have a common bounded support of  $[-1, 1]$ ; that is,  $-1 \leq \zeta^t \leq 1$  for all  $t = 1, \dots, T$ .

Under these assumptions, a conservative substitute of (29) based on moment generating functions is given by [7], [21]

$$\inf_{v>0} [f^0(\mathbf{x}) + v \sum_{t=1}^T \Omega^t(v^{-1} f^t(\mathbf{x})) + v \log(\frac{1}{\epsilon})] \leq 0 \quad (30)$$

where  $v > 0$  is the optimization variable,  $\Omega^t(y) := \max_{\pi^t} \Phi(y)$ , and  $\Phi(y, \pi^t) := \log(\int \exp(xy) d\pi^t(x))$  represents logarithmic moment generation function. Moreover, it is guaranteed that (30) is convex [7], [21]. However, in general,  $\{\Omega^t(y)\}$  may not be easy to evaluate. To this end, one can consider an upper-bound for  $\Omega^t(y)$  given by

$$\Omega^t(y) \leq \max\{\mu_t^- y, \mu_t^+ y\} + \frac{\sigma_t^2}{2} y^2, t = 1, \dots, T \quad (31)$$

where  $\mu_t^-, \mu_t^+$  with  $-1 \leq \mu_t^- \leq \mu_t^+ \leq 1$  and  $\sigma_t \geq 0$  are constants that depend on the given families of probability distributions. Some examples are given in [21, Table 1], where the useful prior knowledge includes the support, unimodality (with respect to the center of the support), and symmetry of the distribution, as well as the ranges of the first- and the second-order moments. Using more prior knowledge leads to tighter approximation. Replacing  $\Omega^t(\cdot)$  in (30) with this upper-bound, and invoking the arithmetic-geometric inequality, yields

$$f^0(\mathbf{x}) + \sum_{t=1}^T \max\{\mu_t^- f^t(\mathbf{x}), \mu_t^+ f^t(\mathbf{x})\} + \kappa \left( \sum_{t=1}^T \sigma_t^2 f^t(\mathbf{x})^2 \right)^{\frac{1}{2}} \leq 0 \quad (32)$$

as a convex conservative surrogate for (29).

Due to the renewable resources generation limits and the fact that the total load of a household or a building is limited, it is natural to assume that the distributions of  $P_{R_{net}}^t$  and  $P_{L_{net}}^t$  have bounded support of  $[l_X^t, u_X^t]$  and  $[l_Y^t, u_Y^t]$ , respectively. Therefore,  $Z^t$  has also a bounded support of  $[l_Z^t, u_Z^t]$ . More specifically, with  $(\sigma_Z^t)^2 := (\sigma_{P_{R_{net}}^t})^2 + (\sigma_{P_{L_{net}}^t})^2$  and  $\mathbb{E}[Z^t] := \hat{Z}^t$  as the nominal value, it is assumed that  $Z^t - \hat{Z}^t \in [-\sigma_Z^t, \sigma_Z^t]$ . Furthermore, in addition to the load and total renewables output generation independence, it is assumed that

the total shortage outputs  $Z^t$  and  $Z^t$  are independent. Let introduce constants  $a_Z^t := \frac{1}{2}(u_Z^t - l_Z^t) = \sigma_Z^t$  and  $b_Z^t := \frac{1}{2}(u_Z^t + l_Z^t) = \hat{Z}^t$  to normalize the supports to  $[-1, 1]$  per as3); that is,

$$\zeta_Z^t := \frac{Z^t - b_Z^t}{a_Z^t} \in [-1, 1]. \quad (33)$$

Then, with (33) and letting

$f^0(S^{max}, \mathbf{P}_{excess}^t, \mathbf{P}_G^t) = -(1 - DoD^{th})S^{max} + S_E^0 + \sum_{t'=1}^t b_Z^{t'} + \sum_{t'=1}^t \sum_{d=1}^D$  and  $f^t(S^{max}, \mathbf{P}_{excess}^{t'}, \mathbf{P}_G^{t'}) = a_Z^{t'}$  for  $t' \in \tau$ , it follows that (29) is equivalent to (25). Thus, substituting these into (29), (25) is replaced by (34).

Similarly, constraints (26), (27), and (28) can be approximated. With  $\mu_t^+ = \mu_t^- := E\{\frac{Z^t - b_Z^t}{a_Z^t} | a_Z^t \leq Z^t \leq b_Z^t\} = 0$  and  $\sigma^t = 1$ , Bernstein approximation of the constraints (25), (26), (27), and (28) boil down to (34), (35), (36), and (37) as shown at the bottom of this page

$$\text{here } \kappa = \sqrt{2 \log \frac{1}{\epsilon'}}.$$

## B. Gaussian Approximation

A yet another approximation can be deployed here to approximate (17), and (18) and avoid conservatism of Bernstein method. The tacit assumption here is that the forecast errors in the load and renewable output power follow a Gaussian distribution, i.e.,  $P_{Rnet}^t \sim N(\hat{P}_{Rnet}^t, (\sigma_{Rnet}^t)^2)$  and  $P_{Lnet}^t \sim N(\hat{P}_{Lnet}^t, (\sigma_{Lnet}^t)^2)$ . Then, it can be shown that approximate constraints through Gaussian approximation are the same as Bernstein approximation except that  $\kappa$  is replaced by  $Q^{-1}(\epsilon')$ , where the  $Q(\cdot)$  is the standard Gaussian tail function.

# SECTION V. The Proposed Algorithm

## A. Robust Algorithm

Substituting the probabilistic constraints and taking the expectation in objective function, the problem (P1) can be re-written as

$$\begin{aligned}
(P2) \min_{S^{max}, P_G^t} & \sum_{t=1}^T \sum_{d=1}^D (a_d P_{G_d}^t + b_d P_{G_d}^t + c) \\
& + \alpha S_{max} + \sum_{t=1}^T \beta_{max}^t \\
& \times [(1 - DoD^{th}) S^{max} + \sum_{t'=1}^t \\
& \times (- \sum_{d=1}^D P_{G_d}^{t'} - \hat{P}_{R_{net}}^{t'} + \hat{P}_{L_{net}}^{t'} + P_{excess}^{t'})] \\
& + \eta^t \sum_{t=1}^T C_Z^t - 2(P_{excess}^t + P_{cap})(\hat{P}_{R_{net}}^t - \hat{P}_{L_{net}}^t) \\
& + (P_{excess}^t + P_{cap})^2 \\
\text{subject to:} & (19), (20), (21), (34), (35), (36), \text{and } (37)
\end{aligned}$$

(38)

**Proposition 1**

If (P2) is feasible, then deploying dual method leads to zero duality gap and global optimum.

**Proof:**

The constraints are linear with respect to  $P_{G_d}^t$ ,  $P_{excess}^t$  and  $S^{max}$ . In addition, the cost function in (P2) consists of continuous quadratic and linear terms which are known to be convex over the entire space. Since the continuous convex cost function in (P2) is minimized over a nonempty compact set specified by the set of constraints in (P2), the optimal value is also finite. These two conditions are sufficient to claim on zero duality gap and the dual method is well motivated [22].

**Remark 2:**

It is worth noting that Bernstein approximation is made conservative in the sense that the feasible set of the approximated problem (P2) is a feasible subset of the original problem (P1). Then, by construction the optimal solution of (P2) is guaranteed to be feasible suboptimal solution for the original problem.

Introducing dual variables  $\mathbf{v} = [v_1, \dots, v_T]$ ,  $\boldsymbol{\lambda} = [\lambda_1, \lambda_2, \dots, \lambda_T]$ ,  $\boldsymbol{\omega} = [\omega_1, \dots, \omega_T]$ ,  $\boldsymbol{\gamma} = [\gamma_1, \dots, \gamma_T]$ , The dual function is given by

$$\begin{aligned}
D(\mathbf{v}, \boldsymbol{\lambda}, \boldsymbol{\omega}, \boldsymbol{\gamma}) &= \inf_{\substack{0 \leq P_{excess}^t, P_G^{min} \leq P_G^t \leq P_G^{max}, 0 \leq S^{max} \leq S^{cap} \\ T}} \\
&\times \sum_{t=1}^T L_1^t(\mathbf{P}_G^t; \mathbf{v}, \boldsymbol{\lambda}, \boldsymbol{\omega}, \boldsymbol{\gamma}) + L_2^t(S^{max}; \boldsymbol{\lambda}) \\
&+ L_3^t(\mathbf{v}, \boldsymbol{\lambda}, \boldsymbol{\omega}, \boldsymbol{\gamma}) + L_4^t(\mathbf{P}_{excess}^t, \mathbf{v}, \boldsymbol{\lambda}, \boldsymbol{\omega}, \boldsymbol{\gamma}) \\
&= \begin{cases} \inf_{P_G^{min} \leq P_G^t \leq P_G^{max}} \sum_{t=1}^T L_1^t + L_3^t + L_4^t \\ \text{if } \lambda^t = \beta_{max}^t + \frac{\alpha}{T(1 - DoD^{th})} \\ -\infty, \text{ otherwise} \end{cases}
\end{aligned} \tag{39}$$

(39)

where

$$\begin{aligned}
L_1^t := & \sum_{d=1}^D a_d P_{G_d}^{t2} + \sum_{d=1}^D b_d P_{G_d}^t \\
& + (\omega^t - \gamma^t) \sum_{d=1}^D P_{G_d}^t + (\lambda^t - \nu^t - \beta_{max}^t) \sum_{t'=1}^t \sum_{d=1}^D P_{G_d}^{t'} \quad (40)
\end{aligned}$$

$$L_2^t = S^{max} \left( (1 - DoD^{th}) \beta_{max}^t + \frac{\alpha}{T} - \lambda^t (1 - DoD^{th}) \right) \quad (41)$$

$$\begin{aligned}
L_3^t = & -2\eta^t P_{excess}^t (\hat{P}_{R_{net}}^t - \hat{P}_{L_{net}}^t) + \eta^t (P_{excess}^t + P_{cap})^2 \\
& - (\omega^t - \gamma^t) P_{excess}^t - (\lambda^t - \nu^t) \sum_{t'=1}^t P_{excess}^{t'} \quad (42)
\end{aligned}$$

$$\begin{aligned}
L_4^t = & \lambda^t (A^t + V^t) - \nu^t (A^t - V^t) + \omega^t (-P_E^{max} + B^t + H^t) \\
& + \gamma^t (P_E^{min} - B^t + H^t) \quad (43)
\end{aligned}$$

and  $A^t := S_E^0 + \sum_{t'=1}^t Z^{t'}$ ,  $V^t := \kappa \left( \sum_{t'=1}^t (\sigma_Z^{t'})^2 \right)^{\frac{1}{2}}$  and  $H^t := \kappa \sigma_Z^t$ . Then, the dual problem is given by

$$\sup_{\mathbf{v} \geq \mathbf{0}, \boldsymbol{\omega} \geq \mathbf{0}, \boldsymbol{\gamma} \geq \mathbf{0}} D(\mathbf{v}, \boldsymbol{\omega}, \boldsymbol{\gamma}) \quad (44)$$

It is interesting to note that the optimization in (39) can be decomposed per time slot, thanks to the separable structure of the problem. Specifically, at each time slot  $t \in \tau$ , the optimal power for generator  $d \in \mathcal{D}$  and optimal excess power are obtained by

$$P_{G_d}^{*t} = \left[ \frac{\gamma^t + \nu^t - \omega^t - b_d + \eta}{2a_d} - \frac{\alpha}{2a_d T(1 - DoD^{th})} \right]_{P_G^{min}}^{P_G^{max}} \quad (45)$$

$$P_{excess}^{*t} = \left[ \frac{\gamma^t + \nu^t - \omega^t - b_d + \eta}{2a_d} - \frac{\alpha}{2a_d T(1 - DoD^{th})} \right]^+ \quad (46)$$

where  $[a]^+ := \max(0, a)$ . It is immediate from (34) that the optimal storage size is given by

$$S^{*max} \geq \frac{A^t + V^t}{(1 - DoD^{th})} + \frac{\sum_{t'=1}^t \sum_{d=1}^D P_{G_d}^{*t'}}{(1 - DoD^{th})}, t \in \tau \quad (47)$$

it then follows

$$S^{*max} = \max_t \frac{A^t + V^t}{(1 - DoD^{th})} + \frac{\sum_{t'=1}^t \sum_{d=1}^D P_{G_d}^{*t'}}{(1 - DoD^{th})} \quad (48)$$

The optimal solution of (44) can be obtained via iterative optimization methods such as the subgradient method, which requires the subgradient of  $D(\cdot)$  w.r.t.  $[\mathbf{v}, \boldsymbol{\omega}, \boldsymbol{\gamma}]$ . The subgradient is as follows

$$g_{\mathbf{v}}^t = -A^t + V^t - \sum_{t'=1}^t \sum_{d=1}^D P_{G_d}^{t'} + \sum_{t'=1}^t P_{excess}^{t'} \quad (49)$$

$$g_{\boldsymbol{\omega}}^t = -P_E^{max} + B^t + H^t + \sum_{d=1}^D P_{G_d}^t - P_{excess}^t \quad (50)$$

$$g_{\boldsymbol{\gamma}}^t = P_E^{min} - B^t + H^t - \sum_{d=1}^D P_{G_d}^t + P_{excess}^t \quad (51)$$

To avoid the computational complexity resulted from the large dimension of the optimization problem due to the use of a large data set of load and renewable power, the original optimization problem is solved in each time slot in a distributed manner. The detailed algorithm is shown in Table I.

**TABLE I** Algorithm for Solving (P2)

1:	Initialize Lagrange multipliers $\mathbf{v}, \boldsymbol{\omega}, \boldsymbol{\gamma}, \eta$ . Set tolerance $\tau$
2:	For $t = 1, \dots, T$ do
3:	Find $P_{G_d}^{*t}$ and $P_{excess}^{*t}$ from (45) and (46)
4:	Repeat $i = 0, 1, 2, \dots$
5:	$\mathbf{v}^{i+l} = \mathbf{v}^i + \eta^i g_{\mathbf{v}}^i,$ $\boldsymbol{\omega}^{i+l} = \boldsymbol{\omega}^i + \eta^i g_{\boldsymbol{\omega}}^i,$ $\boldsymbol{\gamma}^{i+l} = \boldsymbol{\gamma}^i + \eta^i g_{\boldsymbol{\gamma}}^i$
6:	Until convergence
7:	End for
8:	Find $S^{*max}$ from (48)

## B. Simplified Algorithm Incorporating Only the Historical Data

In case the forecast error is not available, one can resort to only forecast data (or historical data), without incorporating the forecast error. Then, the probabilist constraints in (P1) are substituted by the following

$$S_{min} \leq S_E^0 + \sum_{t'=1}^t \mathbb{E}\{U^{t'}\} \leq (1 - DoD^{th})S^{max}, t \in \tau \quad (52)$$

$$P_E^{min} \leq \mathbb{E}\{U^t\} \leq P_E^{max}, t \in \tau \quad (53)$$

where  $\mathbb{E}\{U^t\}$  is obtained from (24) and entails load and renewable forecast power data. Similar to (P2), this optimization problem is convex and can be solved using dual method. The optimal solutions to this problem can be obtained from Table I, where the subgradients are simply obtained by substituting  $\sigma_Z^t = 0$  for  $t \in \tau$  from the following

$$g_v = -S_E^0 + \sum_{t'=1}^t \{-\hat{P}_{R_{net}}^{t'} + \hat{P}_{L_{net}}^{t'} + P_{excess}^{t'}\} - \sum_{t'=1}^t \sum_{d=1}^D P_{G_d}^{t'} \quad (54)$$

$$g_\omega = -P_E^{max} + \hat{P}_{R_{net}}^t - \hat{P}_{L_{net}}^t - P_{excess}^t + \sum_{d=1}^D P_{G_d}^t \quad (55)$$

$$g_\gamma = P_E^{min} - \hat{P}_{R_{net}}^t + \hat{P}_{L_{net}}^t + P_{excess}^t - \sum_{d=1}^D P_{G_d}^t. \quad (56)$$

## SECTION VI. Numerical Tests

In this section the proposed algorithm for generation output power and storage capacity optimization is verified using numerical tests.

### A. Microgrid Without Solar Generation

A microgrid with  $D = 2$  generators,  $R = 3$  wind farms is considered. The hourly wind farms power data for the year 2012 were obtained from three geographically adjacent sites in NREL database [23]. The hourly total forecast load data of 2012 was collected from ERCOT database [24]. The time horizon spans  $T = 24 \times 300 = 7200$  hours. As shown in Fig. 1, the wind power forecast data has been rescaled to the order of 0 to 312 kW and the load data lies in the range of [160, 353]kW. It can be seen that at some intervals wind output power is enough to cover load power demand and in some instances, another source of energy is required. The generators parameters are  $a_1 = 0.08 \left( \frac{\$}{(\text{kW})^2} \right)$ ,  $a_2 = 0.07 \left( \frac{\$}{(\text{kW})^2} \right)$ ,  $b_1 = 0.5 \left( \frac{\$}{\text{kW}} \right)$ ,  $b_2 = 0.3 \left( \frac{\$}{\text{kW}} \right)$ ,  $P_{G_1}^{min} = P_{G_2}^{min} = 0$  and  $P_{G_1}^{max} = P_{G_2}^{max} = 200\text{kW}$ . Unless stated otherwise,  $\alpha = 0.5 \left( \frac{\$}{\text{Wh}} \right)$ ,  $DoD^{th} = 0.1$ ,  $P_{cap} = 0.02 \max(\hat{Z}) = 3 \text{ kW}$

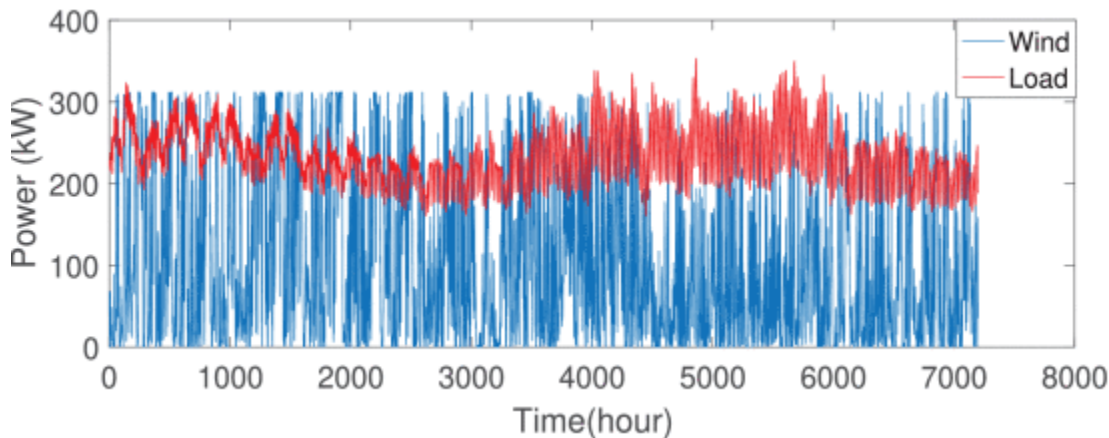
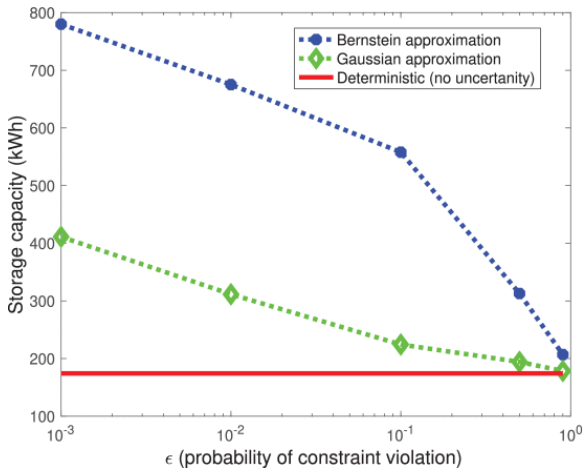


Fig. 1. Load and wind generation hourly data.

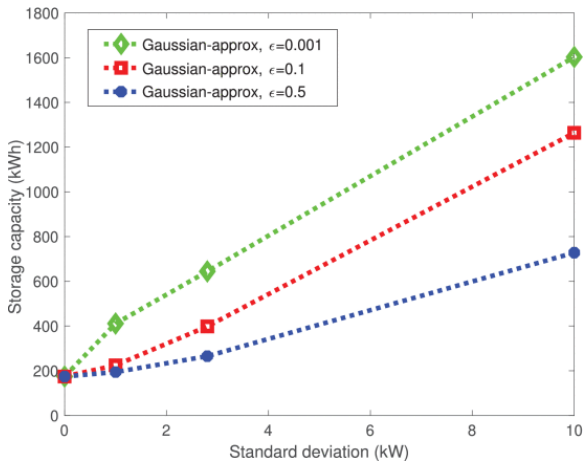
Fig. 2 shows a comparison of the optimal storage capacity for different values of constraints violation probabilistic threshold,  $\epsilon$ , for both Bernstein approximation-based and Gaussian approximation-based algorithms. The solid line without markers is for the case when it is assumed that the standard deviation of forecast error, i.e.,  $\sigma_Z = 0$ , meaning the wind output power and load power shown in Fig. 1 are perfectly known. In this case, the chance constraints boil down to deterministic constraints as detailed in Section V-B and thus the optimal cost and battery capacity do not depend on  $\epsilon$ . The dashed lines with star and diamond markers correspond to the Bernstein approximation-based and the Gaussian approximation-based algorithms, respectively. It can be observed that the optimal storage capacity increases as  $\epsilon$  increases, since larger  $\epsilon$  renders

the chance constraint more lenient. Also, it can be seen that the curves corresponding to the optimal storage capacity through Gaussian approximation-based algorithm are closer to the deterministic case than Bernstein approximation. This really confirms that more prior knowledge on the distribution of the forecast error results in more exact and less conservative optimal solutions. However, if minimal prior knowledge is available, one needs to resort to a more conservative approach.



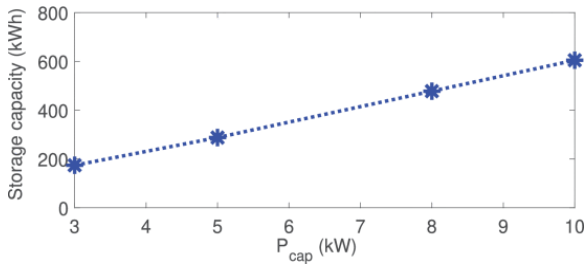
**Fig. 2.** Optimal storage capacity versus probability threshold of constraint violation,  $\epsilon$ .

Fig. 3 shows how prediction error affects on optimal capacity of storage system. The performance of Gaussian approximation-based robust algorithm is compared for different values of  $\sigma_Z$ . The dashed lines with square, star and diamond markers are evaluating Gaussian-based robust algorithm for different values of  $\epsilon$ . It is seen that as the forecast accuracy improves (smaller  $\sigma_Z$ ), the performance of the robust algorithm gets better and eventually touches that of the deterministic case with no uncertainty. In other words, the performance gap will eventually close as  $\sigma_Z$  vanishes. Similar trends are observed for different values of  $\epsilon$ .



**Fig. 3.** Optimal storage capacity versus error standard deviation  $\sigma_Z$ .

The sensitivity of the optimal expected cost to the choice of  $P_{cap}$  is examined in Fig. 4 for deterministic case. It is seen that higher values of  $P_{cap}$ , allows for storage of higher portion of excess wind energy which leads to an increase in storage capacity as well as the total cost.



**Fig. 4.** Optimal storage capacity versus  $P_{cap}$ .

In Fig. 5, the effectiveness of the joint optimal generator and battery power planning for a stable operation of the microgrid is demonstrated. A time horizon of one week is considered. It can be seen that the battery charges when the wind power is beyond the net demand and discharges when the demand exceeds the wind generation. However, due to the cost function for the lifetime of the battery in ( $P1$ ), the algorithm doesn't allow for large variations of the battery energy. Therefore, the trend of charging and discharging of the battery is fairly smooth. As can be seen, the rest of the required power is provided by the generators.

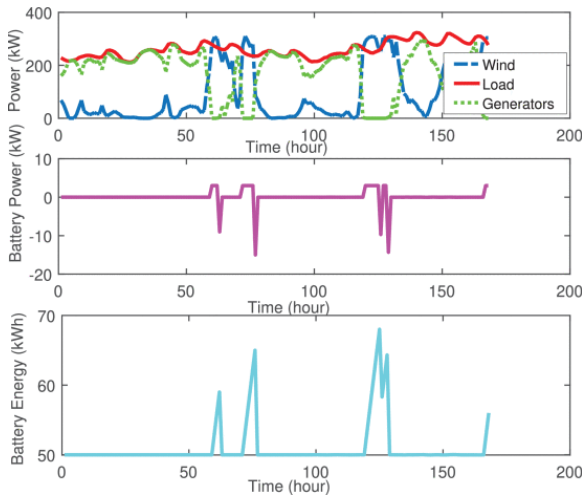


**Fig. 5.** Hourly battery power and energy compared to the load, wind and synchronous generators power.

It is worth noting that as long as ( $P2$ ) is feasible, the algorithm is general enough to accommodate different microgrid scales and similar trends in terms of key conclusions such as the conservatism of approximations, the effect of the approximation error and optimal planning, hold true.

## B. Microgrid with Solar Generation

To validate the proposed algorithms in a more practical setting, Fort Sill microgrid shown in Fig. 6 is considered. It is connected to the utility grid through a 480V/13.20kV transformer and a static switch. The generations in this microgrid include two synchronous generators with the same parameters as previous test except that  $P_{G_1}^{max} = P_{G_2}^{max} = 20 \text{ kW}$ . There is one 90 kW solar PV system, a 50 kW wind turbine, and an energy storage device. The system also includes various motor loads and variable loads. Motor loads mainly include chillers, water pumps, and air compressors. This microgrid can operate in a grid-tie mode or island mode, however, we are interested in island mode in this case study. The same load and wind data from subsection A of numerical tests have been scaled to be used in this microgrid. The solar profile for 24 hours as shown in Fig. 7 has been used to generate solar data for  $T = 2000$  hours.

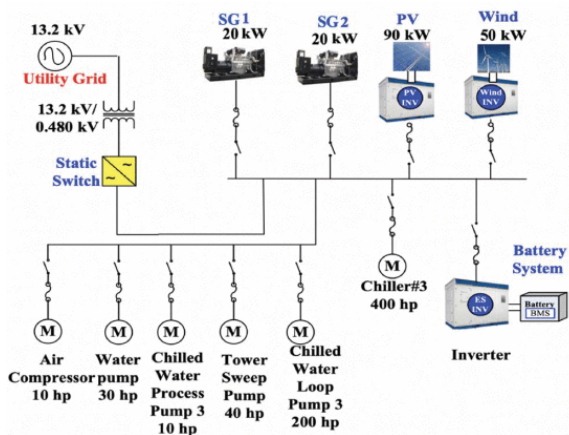


Fig. 6. Schematic of the Fort Sill microgrid.

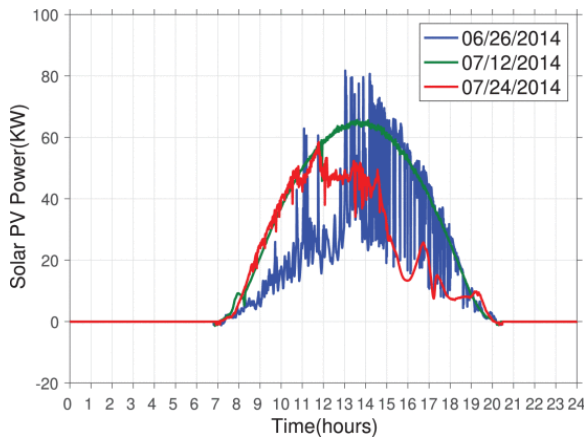


Fig. 7. Solar PV power day profile for a bright day, cloudy day, and the worst power fluctuation during a one-month period.

Similar to Figs. 2 and 3, a comparison of the optimal storage capacity for different values of constraints violation probabilistic threshold,  $\epsilon$ , and standard deviation are shown in Figs. 8 and 9. It can be seen that although the microgrid in the second case includes solar generation and is at a different scale, similar trends hold in both microgrids. Fig. 8 shows that due to lack of distribution assumption and prior knowledge on the uncertainty, the probabilistic constraint is enforced conservatively with Bernstein approximation. However, due to probability distribution assumption, Gaussian approximation provides less conservative solution. In Fig. 9 it can be seen that a large portion of storage capacity estimation error is attributed to the the power output prediction error.

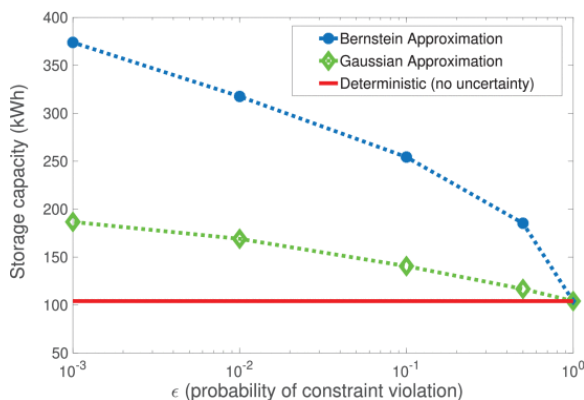
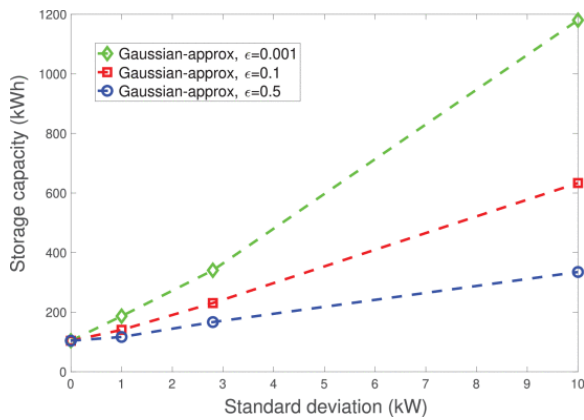


Fig. 8. Optimal storage capacity versus probability threshold of constraint violation,  $\epsilon$ .



**Fig. 9.** Optimal storage capacity versus error standard deviation  $\sigma_z$ .

In addition, the numerical tests illustrate that the size and consequently cost for the energy storage depends on the level of *LOLP* needed for any specific microgrid. For more critical systems, this cost can increase. In an infinite case, the storage must support all the loads for an extended period of time.

It is worth noting that although the algorithm is processing data for  $T$  hours, since the problem is solved per time slot in a distributed manner, it is much faster than processing all the data simultaneously. Using 2.4 GHz 8-Core Intel Core i9 and for  $T = 2000$  hours, the algorithm converges to the optimal solution in 104.815 seconds.

## SECTION VII. Conclusion

Joint storage capacity and generation optimization was considered, where the hourly optimal generation power and storage system capacity were obtained while ensuring that the demand is served with no interruption (demand-balance constraint) and the charging and discharging power of the battery is within the prespecified thresholds. Due to intermittent nature of the load and renewables, the forecast values involve uncertainty and error and the constraints which comprise of renewable generation or load were cast as a chance constraint. As the resulting optimization problem is intractable, two different approaches for approximation were introduced. First, a convex conservative surrogate of the chance constraint was employed using Bernstein approximation, to bypass the need to analytically represent the chance constraint, even without precise knowledge of the distribution of uncertain generation or load. Secondly, assuming that load and generation uncertainty entail Gaussian distribution, an approximation of the chance constraint is obtained. Due to separable structure of the problem, a distributed algorithm based on dual method was proposed. It is worth noting that the conservatism introduced through approximations is a side-effect often shared by a broad class of robust optimization approaches, and arguably constitutes the price paid to obtain guaranteed feasible solutions to chance-constrained problems at an affordable complexity.

## References

1. G. B. Giannakis, V. Kekatos, N. Gatsis, S.-J. Kim, H. Zhu and B. F. Wollenberg, "Monitoring and optimization for power grids: A signal processing perspective", *IEEE Signal Process. Mag.*, vol. 30, no. 5, pp. 107-128, Sep.
2. J. A. P. Lopes, C. L. Moreira and A. G. Madureira, "Defining control strategies for microgrids islanded operation", *IEEE Trans. Power Syst.*, vol. 21, no. 2, pp. 916-924, May 2006.
3. J. M. Carrasco et al., "Power-electronic systems for the grid integration of renewable energy sources: A survey", *IEEE Trans. Ind. Electron.*, vol. 53, no. 4, pp. 1002-1016, Jun. 2006.

4. J. Garcia-Gonzalez, R. de la Muela, L. M. Santos and A. M. Gonzalez, "Stochastic joint optimization of wind generation and pumped-storage units in an electricity market", *IEEE Trans. Power Syst.*, vol. 23, no. 2, pp. 460-468, May 2008.
5. A. Saez-de-Ibarra, A. Milo, H. Gaztañaga, V. Debusschere and S. Bacha, "Co-optimization of storage system sizing and control strategy for intelligent photovoltaic power plants market integration", *IEEE Trans. Sustain. Energy*, vol. 7, no. 4, pp. 1749-1761, Oct. 2016.
6. H. Ibrahim, A. Ilinca and J. Perron, "Energy storage systems—Characteristics and comparisons", *Renew. Sustain. Energy Rev.*, vol. 12, no. 5, pp. 1221-1250, 2008.
7. A. Nemirovski and A. Shapiro, "Convex approximations of chance constrained programs", *SIAM J. Optim.*, vol. 17, no. 4, pp. 969-996, 2006.
8. P. Yang and A. Nehorai, "Joint optimization of hybrid energy storage and generation capacity with renewable energy", *IEEE Trans. Smart Grid*, vol. 5, no. 4, pp. 1566-1574, Jul. 2014.
9. D. Bienstock, M. Chertkov and S. Harnett, "Chance-constrained optimal power flow: Risk-aware network control under uncertainty", *SIAM Rev.*, vol. 56, no. 3, pp. 461-495, 2014.
10. S. Dutta and R. Sharma, "Optimal storage sizing for integrating wind and load forecast uncertainties", *Proc. IEEE PES Innovat. Smart Grid Technol.*, pp. 1-7, Jan. 2012.
11. M. Lubin, Y. Dvorkin and S. Backhaus, "A robust approach to chance constrained optimal power flow with renewable generation", *IEEE Trans. Power Syst.*, vol. 31, no. 5, pp. 3840-3849, Sep. 2016.
12. D. Bertsimas and M. Sim, "The price of robustness", *Oper. Res.*, vol. 52, no. 1, pp. 35-53, 2004.
13. N. Y. Soltani, S.-J. Kim and G. B. Giannakis, "Chance-constrained optimization of OFDMA cognitive radio uplinks", *IEEE Trans. Wireless Commun.*, vol. 12, no. 3, pp. 1098-1107, Mar. 2013.
14. C. Abbey and G. Joos, "A stochastic optimization approach to rating of energy storage systems in wind-diesel isolated grids", *IEEE Trans. Power Syst.*, vol. 24, no. 1, pp. 418-426, Feb. 2009.
15. K. Baker, G. Hug and X. Li, "Optimal storage sizing using two-stage stochastic optimization for intra-hourly dispatch", *Proc. North Amer. Power Symp. (NAPS)*, pp. 1-6, 2014.
16. H. Bludszweit and J. A. Dominguez-Navarro, "A probabilistic method for energy storage sizing based on wind power forecast uncertainty", *IEEE Trans. Power Syst.*, vol. 26, no. 3, pp. 1651-1658, Aug. 2011.
17. H. V. Haghi and S. Lotfifard, "Spatiotemporal modeling of wind generation for optimal energy storage sizing", *IEEE Trans. Sustain. Energy*, vol. 6, no. 1, pp. 113-121, Jan. 2015.
18. P. Harsha and M. Dahleh, "Optimal management and sizing of energy storage under dynamic pricing for the efficient integration of renewable energy", *IEEE Trans. Power Syst.*, vol. 30, no. 3, pp. 1164-1181, May 2015.
19. S. Bayram, M. Abdallah, A. Tajer and K. A. Qaraqe, "A stochastic sizing approach for sharing-based energy storage applications", *IEEE Trans. Smart Grid*, vol. 8, no. 3, pp. 1075-1084, May 2017.
20. Y. Zhang, N. Gatsis and G. B. Giannakis, "Robust energy management for microgrids with high-penetration renewables", *IEEE Trans. Sustain. Energy*, vol. 4, no. 4, pp. 944-953, Oct. 2013.
21. A. Ben-Tal and A. Nemirovski, "Selected topics in robust convex optimization", *Math. Program. B*, vol. 112, no. 1, pp. 125-158, 2008.
22. D. P. Bertsekas, *Constrained Optimization and Lagrange Multiplier Methods*, Belmont, MA, USA:Athena Sci, 1996.
23. C. Draxl, B. M. Hodge, A. Clifton and J. McCaa, "Overview and meteorological validation of the wind integration national dataset toolkit", 2015.
24. *ERCOT Hourly Load Data Archive*, 2012, [online] Available: [http://www.ercot.com/gridinfo/load/load\\_hist/](http://www.ercot.com/gridinfo/load/load_hist/).